Princeton Plasma Physics Laboratory

PPPL- 4859

PPPL- 4859

A Magnetic Diagnostic Code for 3D Fusion Equilibria

Samuel A. Lazerson, S. Sakakibara and Y. Suzuki

March, 2013

PPPL PRINCETON PLASMA PHYSICS LABORATORY

Prepared for the U.S. Department of Energy under Contract DE-AC02-09CH11466.

Princeton Plasma Physics Laboratory
Report Disclaimers

Full Legal Disclaimer

Trademark Disclaimer

PPPL Report Availability

Princeton Plasma Physics Laboratory:

http://www.pppl.gov/techreports.cfm

Office of Scientific and Technical Information (OSTI):

http://www.osti.gov/bridge

Related Links:

U.S. Department of Energy

Office of Scientific and Technical Information

Fusion Links

A Magnetic Diagnostic Code for 3D Fusion Equilibria

‡

S.A. Lazerson

Princeton Plasma Physics Laboratory, Princeton, NJ

E-mail: lazerson@pppl.gov

S. Sakakibara and Y. Suzuki

National Institute for Fusion Science

Abstract.

A synthetic magnetic diagnostics code for fusion equilibria is presented. This code calculates the response of various magnetic diagnostics to the equilibria produced by the VMEC and PIES codes. This allows for treatment of equilibria with both good nested flux surfaces and those with stochastic regions. DIAGNO v2.0 builds upon previous codes through the implementation of a virtual casing principle. The code is validated against a vacuum shot on the Large Helical Device (LHD) where the vertical field was ramped. As an exercise of the code, the diagnostic response for various equilibria are calculated on the LHD.

PACS numbers: 52.55.-s,52.55.Hc,52.70.Ds,28.52.Av

Keywords: Fusion, Magnetics, Diagnostics, Equilibria, Reconstruction

Submitted to: *Plasma Phys. Control. Fusion*

 The authors would like to thank the LHD experiment group and the technical staff in LHD for their support of this work. This work is partly supported by the National Institute for Fusion Science grant administrative budgets (NIFS07KLPH004).

1. Introduction

The calculation of synthetic magnetic diagnostics for three dimensional magnetic fields in fusion devices is important for both stellarator and tokamaks with non-axisymmetric field coils. The single helicity state in reverse field pinches also requires a 3D treatment [1]. Simulation of magnetic signals for two-dimensional toroidal configurations is a well treated problem in magnetically confined fusion. This has allowed for the development of codes which fit magnetic equilibria to various plasma diagnostics [2, 3]. Three dimensional fields require significantly larger computational efforts to achieve similar goals. Thus only devices which had inherently three-dimensional fields (stellarators and heliotrons) required these more computationally expensive codes. It has now been recognized that otherwise axisymmetric configurations can benefit from three-dimensional fields [4, 5] motivating the development of computational tools capable of handling such configurations. Recent work on edge localized modes suggest that 3D physics plays an important role in future fusion devices such as ITER. The code presented in this paper, DIAGNO v2.0, interfaces with both the VMEC [6] and PIES [7] codes to calculate the magnetic diagnostic response to their three dimensional equilibria. The VMEC code assumes that a set of nested flux surfaces fill the plasma volume. The PIES code make no such assumption and calculates the location of islands and stochastic regions through field line following. This allows these 3D equilibrium codes to be used for reconstruction purposes. This code also allows for the examination of magnetic diagnostic response to islands and stochastic regions. Previous diagnostic codes were only coupled to equilibrium codes which did not posses such features (VMEC) or lacked the ability to simulate the total diagnostic response (EXTENDER) [7].

The development of this code was necessitated by limitations present in the original DIAGNO code [8] and the development of more generalized methods for treating problem of calculating the plasma response from a given equilibrium. The DIAGNO code calculated the plasma response of the magnetic field (external to the plasma) using three pieces of information (from VMEC): a potential on the equilibrium surface, a current placed on the magnetic axis, and the vacuum field on the surface (via Biot-Savart's law). The scalar potential placed on the plasma boundary limited the applicability of the method to the VMEC code. The use of Biot-Savart's law made the calculation grow as the size of the field coil detail. Recently a code was developed which utilized a virtual casing principle [9, 10] allowing for the calculation of the external magnetic field with only the specification of the plasma boundary and the magnetic field on that boundary (EXTENDER). As DIAGNO could already handle the details of calculating various diagnostic responses, the decision to modify the DIAGNO code to calculate external fields using a virtual casing principle was made. Here the diagnostic response is calculated via a surface integral over the plasma boundary as opposed to codes which conduct a volume integral over plasma currents (V3FIT [11] and JDIA [12, 13]). The utility of virtual casing greatly extends the applicability of DIAGNO to multiple codes. Any code which outputs a magnetic field on a surface (at the plasma

edge or outside the plasma) can now be interfaced to DIAGNO.

This paper discusses the DIAGNO v2.0 code along with providing a benchmark against a vacuum shot on the Large Helical Device (LHD). The LHD is a ten field period helical fusion device with superconducting coils which has been in operation in Japan since 1998 [14]. The major radius of the device is 3.9 $[m]$ with average minor radius of 0.6 $[m]$, with volume average plasma betas ($< \beta >$) of up to 5%. The set of magnetic diagnostics on LHD, previously calibrated using the JDIA code, provides an excellent test case for the DIAGNO v2.0 code [15]. Section 2 discusses the methodology of the code. Details of it's calculation of the field on the equilibrium boundary are provided for both VMEC and PIES equilibria. Section 3 compares the calculations against a vacuum shot on LHD and examines the diagnostic response to finite β equilibria. Section 4 summarizes the results.

2. Method

The DIAGNO v2.0 code employs a virtual casing principle to calculate the fields external to a given plasma equilibrium. This allows the calculation of the magnetic plasma response with only the knowledge of the total magnetic field on the boundary, providing a very simple interface to many existing codes. Additionally, the code can also do a direct Biot-Savart calculation of the diagnostic response due to field coil energization. This allows for a calculation of a mutual inductance matrix for all diagnostics. The Biot-Savart calculation is performed using a method utilized in many other fusion codes [16]. This method utilizes a compact expression for the Biot-Savart magnetic field and vector potential which is singular only on the line segment. The code is currently designed to calculate the diagnostic response of magnetic field probes, flux loops, diamagnetic loops, segmented Rogowski coils, and Mirnov arrays.

The previous version of the code did not have such utility. The original version of DIAGNO utilized quantities calculated by the free boundary solver in VMEC. This implied that the code could only be used with free boundary runs of VMEC. Additionally, as VMEC was upgraded and modified, the necessary VMEC output was no longer available. The original code could not calculate mutual inductances between the coil system and diagnostics. The methodology by which plasma response was calculated also limited it to interfacing with the VMEC code alone. These limitations have been removed through modification of the code and utilization of a virtual casing principle for the calculation of plasma response. As a by-product, for machines with detailed coil sets, the execution time of the code has been drastically reduced.

At the numerical boundary between the plasma and vacuum the magnetic field must obey

$$\hat{n} \times \left(\vec{B}_{out} - \vec{B}_{in} \right) = \mu_0 \vec{K}_{surf}, \tag{1}$$

where $\hat{n}$ is the surface normal vector pointing from the boundary (in) to the vacuum region (out), $\vec{B}$ is the total magnetic field, μ_0 is the permeability of free space, and $\vec{K}$ is

a surface current density. If this surface is a flux surface then the solenoidal constraint is identically satisfied ($\nabla \cdot \vec{B} = 0$). This is true of codes such as VMEC. There a set of nested flux surfaces is assumed to fill the volume of the plasma. For codes in which the boundary is not a flux surface, such as PIES, a dipole moment density (σ_{dipole}) must also be included. The PIES code calculates flux surface location through field line following on a background coordinate grid. Plasma response is then calculated on this background grid. The radial coordinate grid no longer represents a flux surface allowing for a finite normal component of the magnetic field. This requires a dipole moment density to be present at the boundary. This scalar quantity can be calculated from

$$\left(\vec{B}_{out} - \vec{B}_{in}\right) \cdot \hat{n} = \mu_0 \sigma_{dipole}. \tag{2}$$

As we are concerned with only the plasma response, the external field may be assumed to be zero ($B_{out} = 0$). This is the superconducting shell argument. The source terms for the external field (due to the plasma) become

$$\vec{K}_{surf} = \frac{1}{\mu_0} \vec{B}_{surf} \times \hat{n} \tag{3}$$

and

$$\sigma_{dipole} = -\frac{1}{\mu_0} \hat{n} \cdot \vec{B}_{surf}. \tag{4}$$

The surface current ($\vec{K}$) and dipole density (σ_{dipole}) are then integrated over the plasma surface to find either the magnetic field

$$\vec{B}\left(\vec{x}\right) = \frac{\mu_0}{4\pi} \int \frac{\vec{K}' \times \left(\vec{x} - \vec{x}'\right)}{\left|\vec{x} - \vec{x}'\right|^3} dA' + \frac{\mu_0}{4\pi} \int \frac{\sigma'_{dipole} \left(\vec{x} - \vec{x}'\right)}{\left|\vec{x} - \vec{x}'\right|^3} dA' \tag{5}$$

or vector potential

$$\vec{A}\left(\vec{x}\right) = \frac{\mu_0}{4\pi} \int \frac{\vec{K}'}{\left|\vec{x} - \vec{x}'\right|} dA' + \frac{\mu_0}{4\pi} \int \frac{\sigma'_{dipole}}{\left|\vec{x} - \vec{x}'\right|} \hat{n} dA' \tag{6}$$

at some point in space ($\vec{x}$). In both equations the prime ($'$) denotes quantities on the boundary surface and integration is carried out over the entire surface. The diagnostic response of line integrated signals (flux loops and Rogowski coils) are handled by a variety of line integrated options including multi-step midpoint rule, Bode, and Simpson's rule integration methods.

The DIAGNO v2.0 codes performs these calculations on a gridded mesh on the plasma surface. The VMEC and PIES codes provide Fourier representations of the surface, and fields which are converted into cartesian coordinates. This provides a simple method for specifying the location and orientation of the diagnostics relative to the plasma. The user may specify the number of poloidal and toroidal (per field period) grid points to use in the representation of the surface. The user may also specify the methodology they wish to use for integrated quantities (such as the flux loops response $\int \vec{A} \cdot \vec{dl}$). Available integration methods include midpoint, Simpson and Bode. For the flux loops of the LHD little difference between methods is present. Sensitivity to integration method will depend detail of the diagnostic coil description. The user may

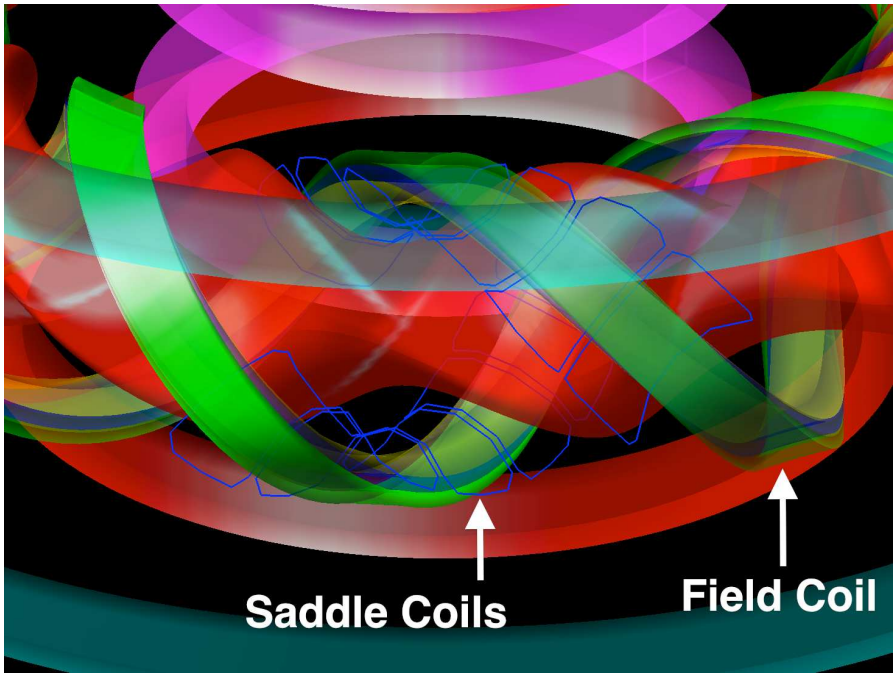

Figure 1. Saddle loops on the Large Helical Device. One of two saddle loop arrays on the LHD (blue lines). A sample equilibrium plasma surface is depicted in red. The multi-layer helical coils is depicted in yellow, blue, and green. Coils providing vertical field are depicted in red, teal, and pink.

specify the number steps to take per line segment for the given integration method. This addresses the integration needs for coils which lack sufficient detail in their description as a set of points in space.

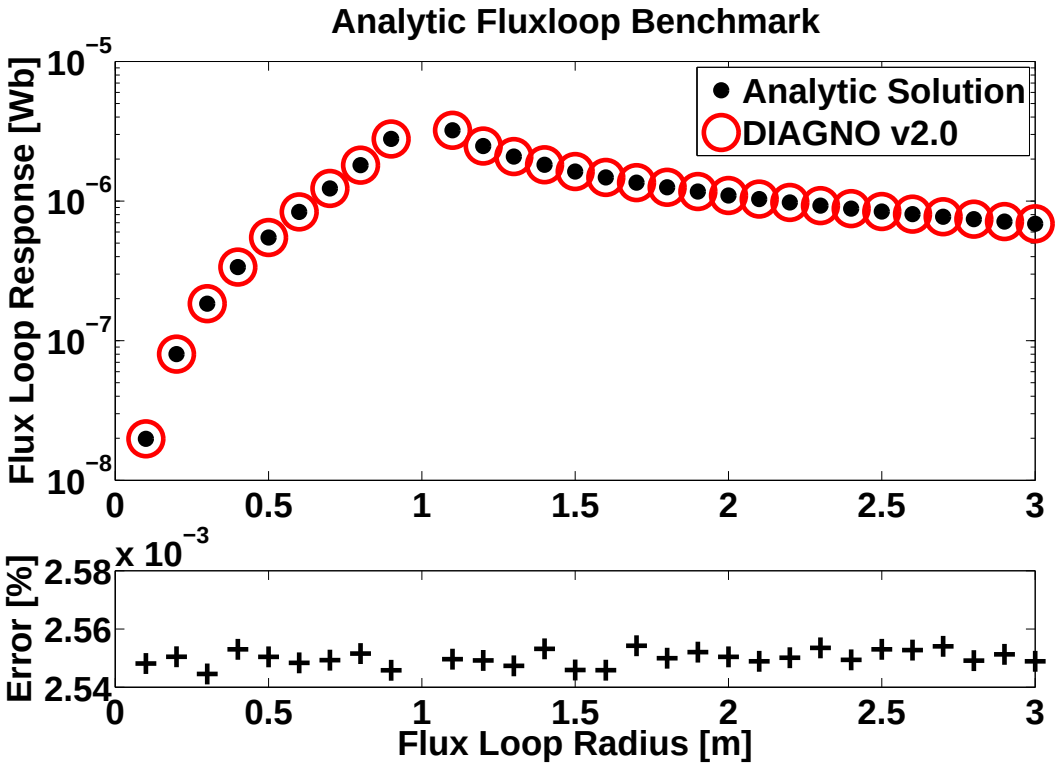

Figure 2. Comparision of DIAGNO v2.0 calculated flux loops responses and analytic estimates. The fluxloop response due to a current carrying ring of radius 1.0 $[m]$ is evaluated for a series of flux loops, concentric with the field ring. Comparison with analytic theory shows errors less than 0.003%.

3. Results

The LHD provides an excellent geometry in which to test the DIAGNO v2.0 code. The helical plasma and 24 saddle type flux loops provide a highly three dimensional configuration (Figure 1). A vertical field ramp (with no plasma) provides a test of the codes ability to calculate diagnostic signals. Tests were conducted between the code and EXTENDER where the field was computed at various points in space for a series of equilibria. These tests show the codes agreed to within a few percent at finite β. A series of equilibria at varying β and net toroidal current were calculated for the LHD. These equilibria provide a gauge of the sensitivity of the DIAGNO v2.0 code to plasma parameters.

The analytic field of a current carrying loop of wire was used to benchmark the ability of the code to calculate mutual inductances between the coils and diagnostics. The diagnostic response of a set of flux loops in the plane of a circular field loop were calculated. Here the vector potential can be expressed (in spherical coordinates) in term

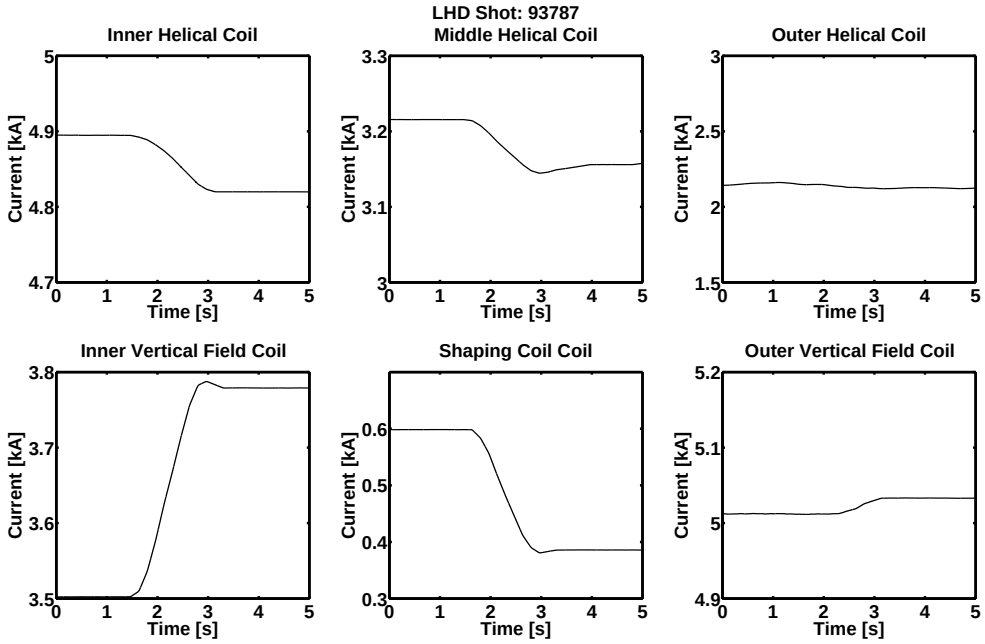

Figure 3. Vacuum shot coil currents on the LHD. The vertical field coils (Outer, Shaping, Inner) indicate a ramp in current around 2.0 $[s]$ into the shot. The helical coil shows some signs of ramping during this time as well. The outer helical coil shows a significant amount of noise when compared to the other coils. However, the calculated mutual inductances indicate a greater sensitivity to the noise in the outer vertical field coil.

of elliptic integrals with the form:

$$A_\phi(r,\theta) = \frac{\mu_0}{4\pi}\frac{4Ia}{\sqrt{a^2+r^2+2ar\sin\theta}}\left[\frac{(2-k^2)K(k)-2E(k)}{k^2}\right] \tag{7}$$

where a is the radius of the coil, μ_0 is the permittivity of free space, I is the coil current, K is the complete elliptic integral of the first kind, E is the complete elliptic integral of the second kind, and the argument k is defined as

$$k^2 = \frac{4ar\sin\theta}{a^2+r^2+2ar\sin\theta}. \tag{8}$$

Figure 2 shows good agreement between analytic theory and the calculated flux loop response for these loops. This test provides an analytic benchmark of the codes ability to calculate the diagnostic responses.

A vertical field ramp was performed in the LHD with no plasma present. This vertical field ramp moved the magnetic axis from a position of ~ 3.55 $[m]$ to ~ 3.60 $[m]$ along the major radius, no vertical movement was indicated. The measured currents in the superconducting coils can be seen in Figure 3. Here the ramp in vertical field coils is clear around 2.0 $[s]$ into the shot. The DIAGNO v2.0 code was utilized the calculate the mutual inductance matrix (between each field coil and each saddle loop). Each saddle loop shows a significantly larger sensitivity to the outer vertical field coil

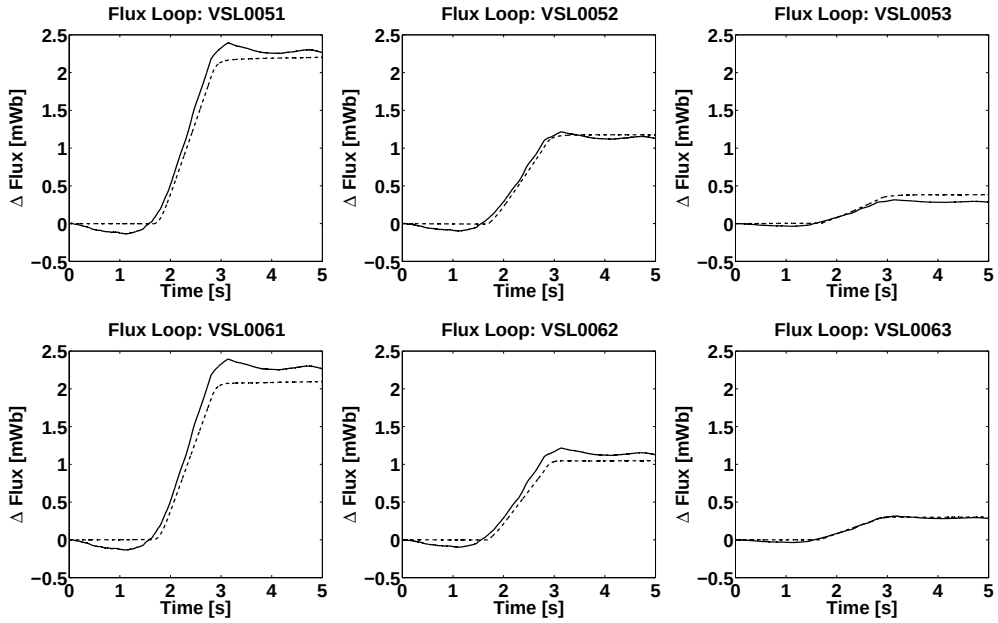

Figure 4. Measured (dashed line) and calculated flux (solid line) through six of the 24 saddle loops on the LHD. Good agreement between calculated and measured signals indicates that the integration of the diagnostic signal around the flux loops is correct.

when compared to the others. A direct calculation of the vacuum flux through each loop is plotted against the measured change in flux (Figure 4). General agreement between measured and calculated change in flux can be seen in the plot. The other 18 saddle loops show similar features. High frequency noise in the outer vertical field coil and outer helical coil were present in the measured coil currents. This contributes to the majority of noise seen in the calculated response. The experimentally measured flux does not posses this noise signal as the integration averages over the high frequency noise. Calculation of the error arising from the noise in the coil currents are of the order of the initial offset between calculated and measured fluxes. This capability of the code to calculate mutual inductance also allows for calibration of flux loop signals.

As the DIAGNO v2.0 code was under development, tests were performed to verify the integrity of the virtual casing principle. The code was debugged through comparisons with the EXTENDER code (which also employs a virtual casing principle, but does not calculate diagnostic response). The field produced by the plasma was evaluated at 29 points around the machine (Figure 5), which correspond to the locations of various magnetic field probes around the LHD, at various volume averaged plasma betas ($< \beta >$). A comparison of the $\hat{z}$ component of the field is shown in Figure 6. This component was chosen as DIAGNO v2.0 outputs the cartesian components of the field and EXTENDER outputs the cylindrical components of the field. This allows for a direct comparison of values output by the codes. Even at low β (and thus low plasma response) both codes agree well within typical measured experimental accuracies. In

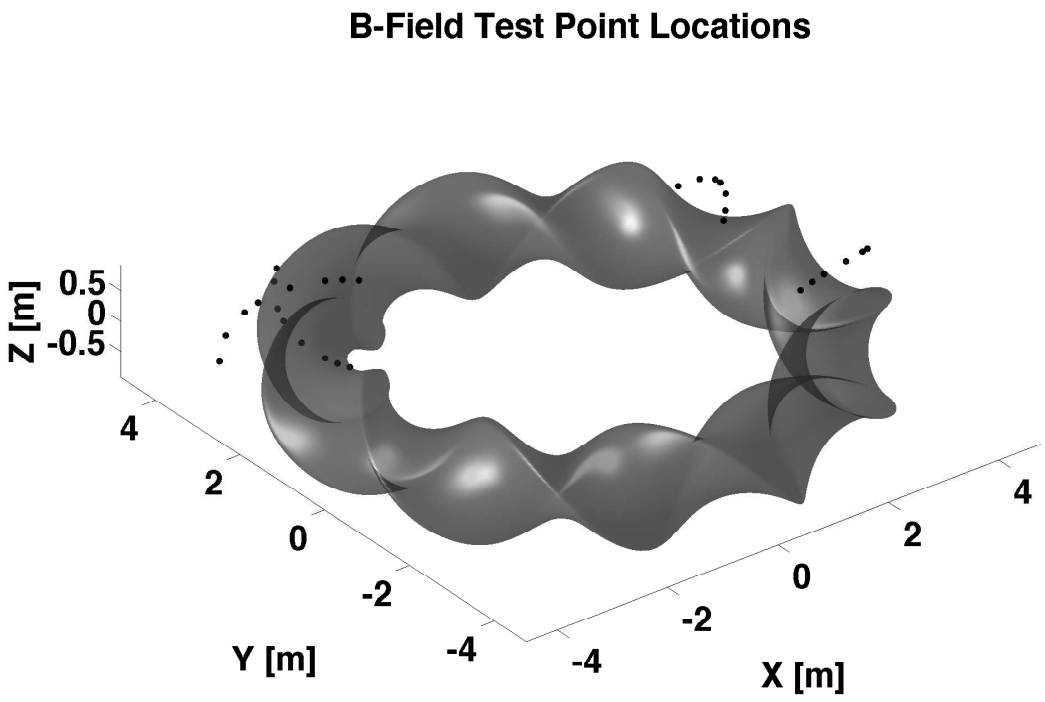

Figure 5. Location of magnetic probes used to benchmark the DIAGNO v2.0 and EXTENDER codes (black dots). The plasma of the LHD at finite β, as calculated by the VMEC code, is shown in grey.

these cases the surface of the plasma was represented by 360 points in the poloidal direction and 360 points in the toroidal direction (over the whole plasma). Comparisons between the original DIAGNO code (at zero net toroidal current) and the new version also show good agreement. Here the speedup associated with the virtual casing principle was clearly evident as the original code ran for 10 minutes and the new code runs in 20 seconds on a single CPU. This is associated with not having to calculate the total field on the surface of the plasma from the field coils. The evaluation of the field due to the coil system scales as the detail of the coil system. For the LHD coil system over $750,000$ data points are evaluated to get the field at a point in space.

A benchmark with the PIES code was also preformed. Here an LHD equilibria at finite β ($\sim 1\%$) and toroidal current (~ 40 $[kA]$) was calculated with VMEC and utilized as an initial condition for the PIES code. The response of the magnetic probes were calculated to benchmark the DIAGNO v2.0 against PIES equilibria. This validates the surface dipole term necessary when calculating the response of PIES equilibria (due to finite normal field on the boundary). Good agreement between EXTENDER and DIAGNO v2.0 can be seen in Figure 7. As a point of interest the diagnostic response

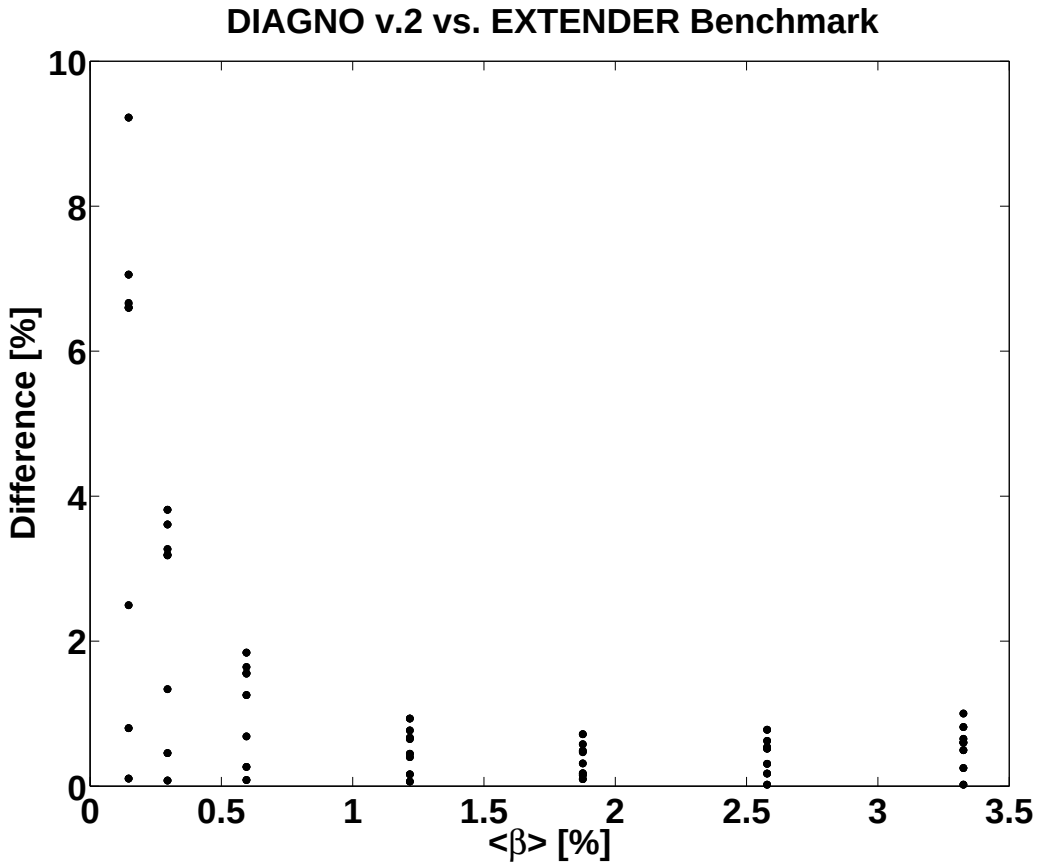

Figure 6. Comparison between vertical magnetic field components (B_Z) calculated by DIAGNO v2.0 and EXTENDER. Agreement between the codes is good even for relatively low $< \beta >$ plasmas (low plasma response).

of the initial VMEC equilibria was also calculated with DIAGNO v2.0. While not all probes detected significant differences in the vertical component of the field, a response associated with the breaking of flux surfaces is clearly evident. It can be noted that differences in the simulated magnetic field ($\sim 50\%$) are large enough to discern against experimental noise. It should be noted that the HINT2 code [17, 18] and the JDIA code have also been interfaced allowing similar calculations to be preformed with different techniques. A more detailed study of the plasma response due to islands and stochastic regions is left to future work.

Parameter sweeps were performed of the plasma $< \beta >$ (volume averaged plasma beta) and net toroidal current. The first test involved calculating a series of equilibria on the LHD where the toroidal current was fixed at zero and plasma β was varied. In the second test, the plasma β on axis was held fixed ($\beta_{axis} \sim 1\%$, $< \beta > \sim 0.6\%$) and the toroidal current was varied. In each case the profiles were assumed to be of a form $f(\Phi) = f_0 (1 - \Phi)^2$ (here Φ is normalized toroidal flux). In these these tests a high field coil energization was assumed (maximum current in each field coil). This provides a method for examining the contribution to diagnostic responses due to finite β and net

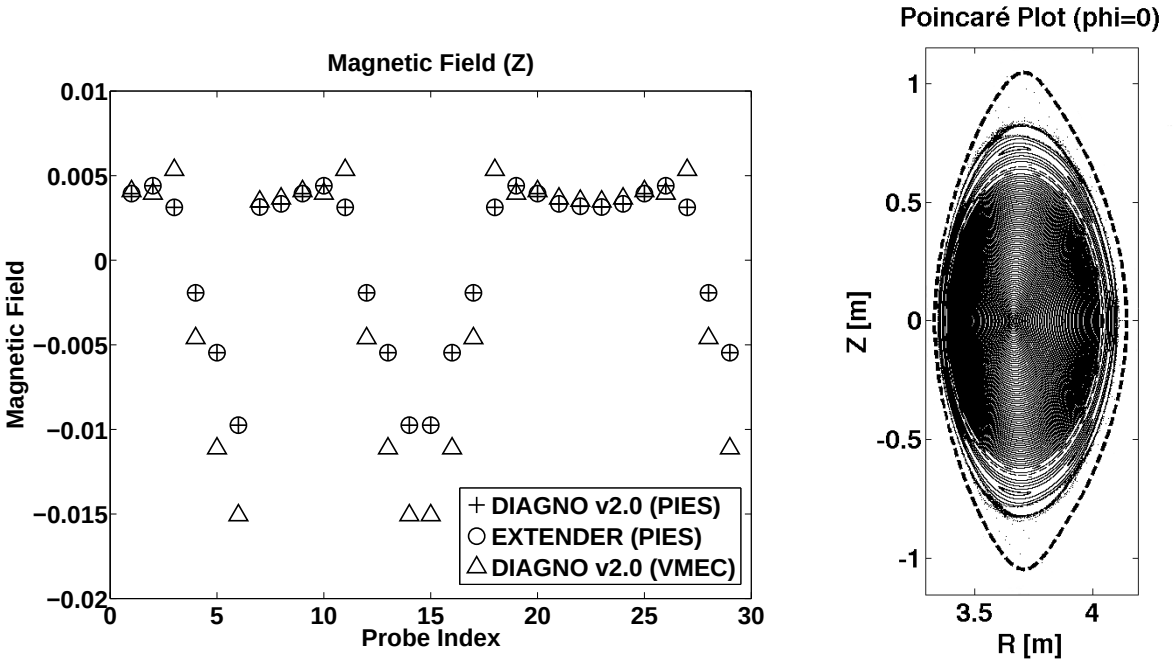

Figure 7. Comparison between vertical magnetic field components (B_Z) calculated by DIAGNO v2.0 and EXTENDER for a PIES equilibria (left) and Poincaré plot for the PIES equilibrium (right). The colocation of the open circles and crosses indicates good agreement between the two codes. Triangles indicate the response associated with the VMEC equilibria used to initialize the PIES run. A dashed line is drawn at the VMEC boundary on the Poincaré plot showing a significant stochastic region at the plasma edge.

toroidal current effects. This is important as the highly three dimensional structure of the plasma and diagnostics makes a-priori assumptions difficult. Additionally, DIAGNO has already been interfaced to equilibrium reconstruction codes. Thus a sensitivity study of the magnetic diagnostics to variations in equilibrium parameters is useful.

The plasma beta on axis (β_{axis}) was varied from vacuum to 0.05 and equilibria were calculated with VMEC. Figure 8 shows the variation in the pressure driven toroidal currents for two choices of β. Here we see that even for modest choices of plasma β current densities on the order of 50 $[kA/m^2]$ are generated. As $< \beta >$ is increased the inboard currents become more localized in the poloidal direction while the outboard currents become more radially localized. Strong Pfirsch-Schlüter resonances in the toroidal current are present in the high β case (radially localized current sheets toward the edge of the plasma) along with significant distortions of the plasma boundary shape. This suggests the presence of islands and stochastic regions in the plasma. The plasma response in the saddle loops are indicated in figure 9. The simulated diagnostic responses are of the order of those measured during experimental campaigns. The response in the saddle loops is nearly linear for all 24 loops. Additionally, a significant amount of redundancy is present in the saddle loop system, as is evident by the overlap of measurements and 10 distinct responses. Comparisons against varying toroidal current

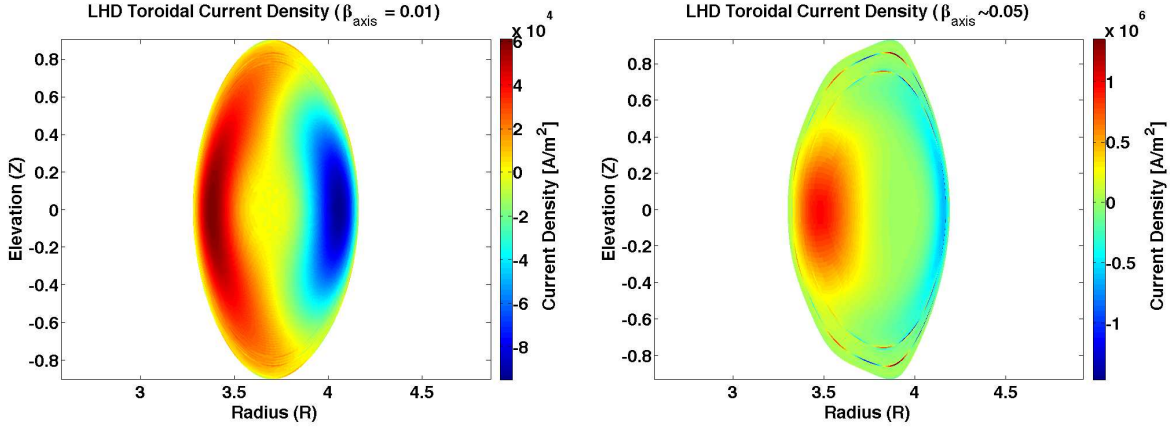

Figure 8. Toroidal current for $\beta_{axis} = 0.01$ (left) and $\beta_{axis} = 0.05$ (right). Pressure driven current densities on the order of 50 $[kA/m^2]$ are present for the $\beta_{axis} = 0.01$ case. The $\beta_{axis} = 0.05$ shows pressure driven current densities on the order of a 1 $[MA/m^2]$. Thin radially localized current sheets are present at the rational surfaces in the plasma.

at finite β were made next.

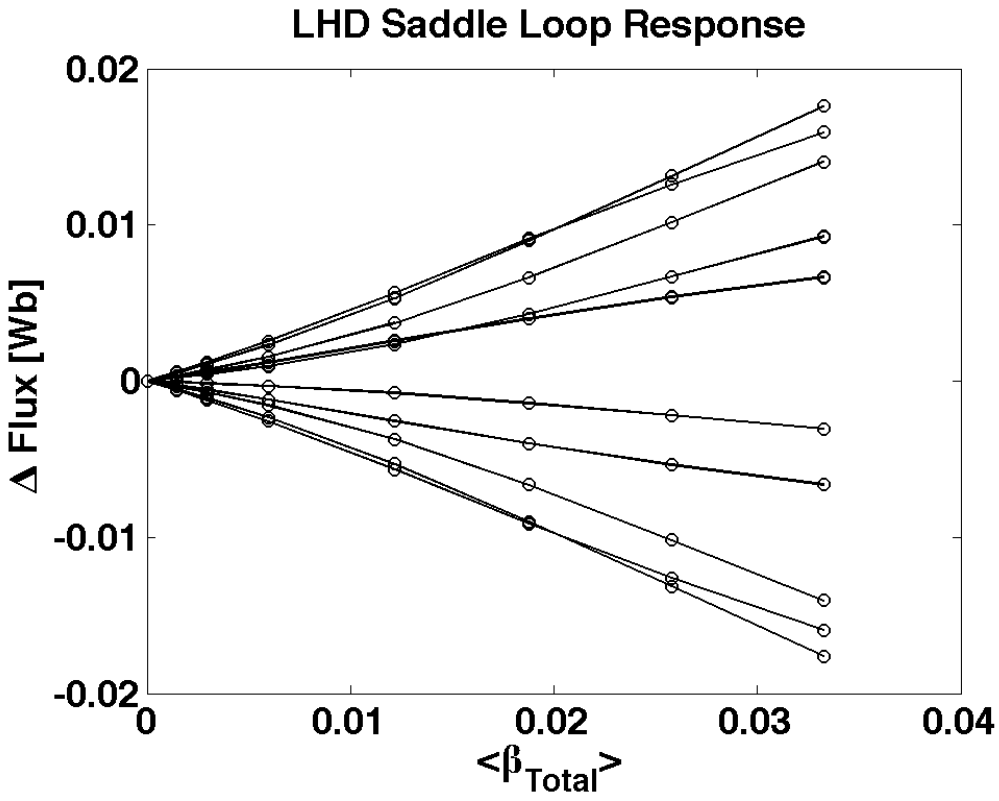

Figure 9. LHD saddle loop response to volume averaged plasma beta ($< \beta_{total} >$). Equilibria were calculated under the assumption of no net toroidal current and a high-field configuration. All 24 loops show a sensitivity to changes in plasma β. These changes are on the order of those recorded in experimental results. As only 10 distinct line are visible in this plot, a significant amount of redundancy is present in the LHD saddle loop diagnostics.

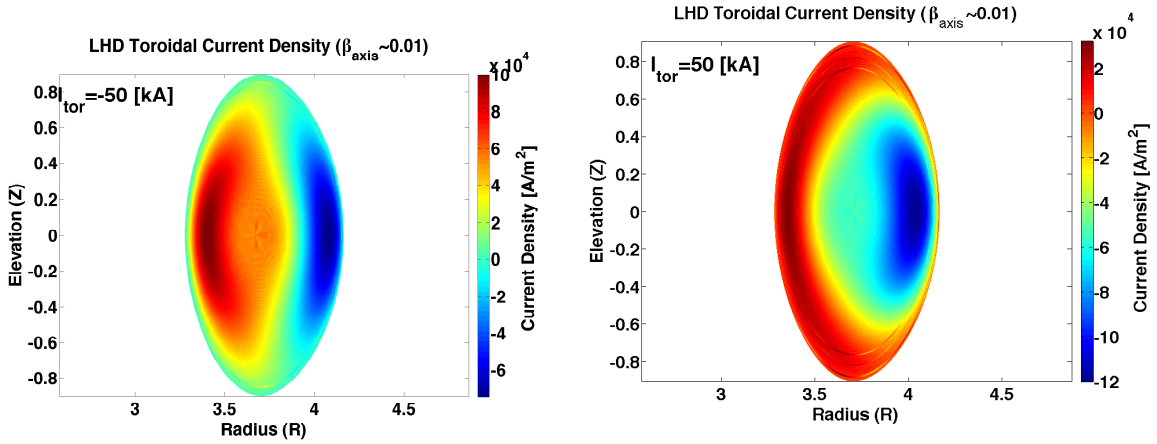

Figure 10. Torodial current for net toroidal current of -50 (left) and 50 $[kA]$ (right) at fixed β. The distribution of toroidal current is clearly modified. Note that positive values are in the negative ϕ direction.

The toroidal current was varied holding the pressure profile fixed ($\beta_{axis} = 0.01$). Figure 10 shows the effect of the toroidal current on current densities at -50 and 50 $[kA]$. The currents associated with finite β are clearly being modified by the net toroidal current. Plots of the diagnostics response show signals (Figure 11) on the order of those generated by finite β effects alone (over a range of -100 to 100 $[kA]$). This equates to the total toroidal current accounting for up to $\sim 40\%$ of the diagnostic signal at a plasma β of ~ 0.01. This indicates that the saddle loops are much more sensitive to the pressure driven currents (and thus β) than net toroidal currents in the plasma. Additionally, the redundancy in the saddle loops for detection of net toroidal current at finite β is even worse with ~ 5 distinct responses in the saddle loop system. Such redundancy can provide valuable information regarding error fields when utilized for equilibrium reconstruction.

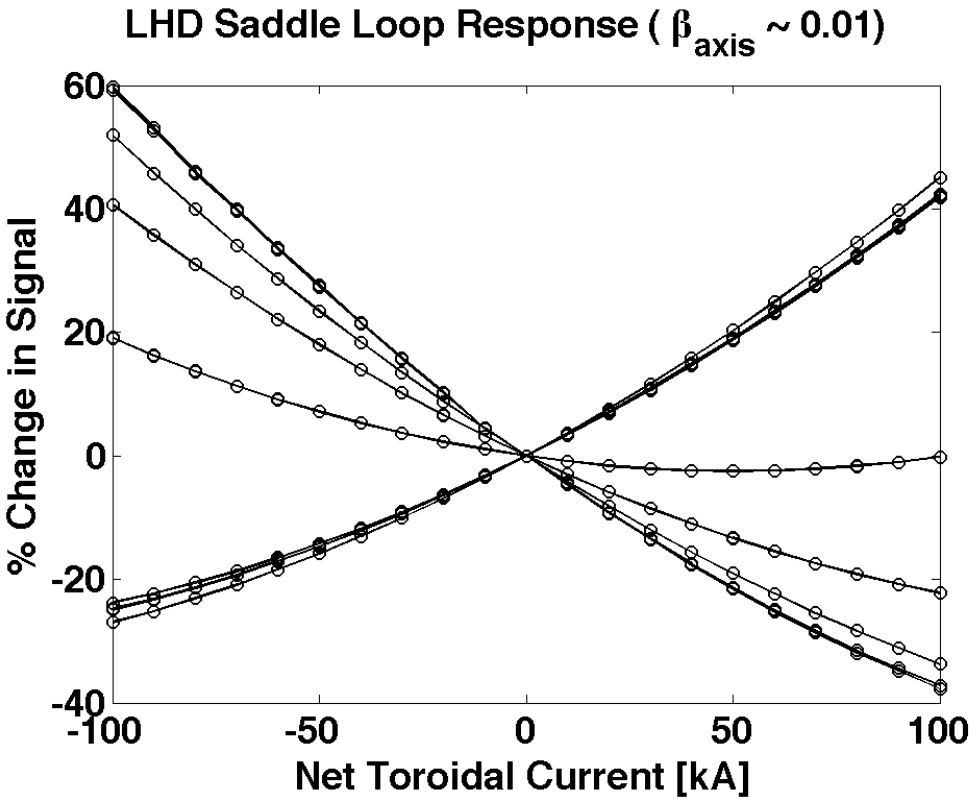

Figure 11. LHD saddle loop response to toroidal current (at finite β). Values have had the finite β signals removed. Equilibria were calculated under the assumption of a plasma β on axis of 1%. Changes in diagnostic signal due to plasma currents are on the order of diagnostic signals due to finite β effects. Redundancy in the saddle loop signals is present as the response of all 24 saddle loops are plotted with only ~ 5 distinct responses (lines).

4. Discussion

A new code, DIAGNO v2.0, has been developed for the calculation of magnetic diagnostic response to 3D equilibria. This code is capable of treating both equilibria generated by the VMEC and PIES codes through a virtual casing principle. This allows for calculation of the effects of islands and stochastic regions on magnetic signals (through PIES equilibria). The virtual casing principle has the added benefit of significant speed enhancements for some magnetic configurations (as compared to the previous code). The code no longer requires a costly evaluation of the vacuum field on the plasma surface. The utility of the code is further extended through it's ability to calculate magnetic signals directly from the field coils. The DIAGNO v2.0 code allows for development of equilibrium reconstruction capabilities for magnetically confined plasmas with 3D fields and extends the reconstruction effort to codes which allow for the formation of magnetic islands and stochastic regions. Finally, the virtual casing principle employed allows for interface with any code which outputs the magnetic field on a toroidal 3D surface. This includes many transport and equilibrium codes currently available.

Acknowledgments

The author would like to thank M. Drevlak for access to the EXTENDER code, H. Gardner for access to the DIAGNO code, S. Hirshman for access to the VMEC code, and A. Reiman for access to the PIES code. The author would also like to thank the LHD Experimental Group for access to the LHD device and data. Finally, the author would like to thank J. Geiger, N. Pomphrey, and D. Monticello for their helpful commentary.

[1] R. Lorenzini, D. Terranova, A. Alfier, P. Innocente, E. Martines, R. Pasqualotto, and P. Zanca. Single-Helical-Axis States in Reversed-Field-Pinch Plasmas. *Phys. Rev. Lett.*, 101:025005, 2008.

[2] L.L. Lao, H. St. John, R.D. Stambaugh, A.G. Kellman, and W. Pfeiffer. Reconstruction of current profile parameters and plasma shapes in tokamaks. *Nucl. Fusion*, 25:1611, 1985.

[3] Q. Peng, J. Schachter, D.P. Schissel, and L.L. Lao. Iefit-an interactive approach to high temperature fusion plasma magnetic equilibrium fitting. In *Real Time Conference, 1999. Santa Fe 1999. 11th IEEE NPSS*, pages 388 –391, 1999.

[4] T. E. Evans, R. A. Moyer, P. R. Thomas, J. G. Watkins, T. H. Osborne, J. A. Boedo, E. J. Doyle, M. E. Fenstermacher, K. H. Finken, R. J. Groebner, M. Groth, J. H. Harris, R. J. La Haye, C. J. Lasnier, S. Masuzaki, N. Ohyabu, D. G. Pretty, T. L. Rhodes, H. Reimerdes, D. L. Rudakov, M. J. Schaffer, G. Wang, and L. Zeng. Suppression of Large Edge-Localized Modes in High-Confinement DIII-D Plasmas with a Stochastic Magnetic Boundary. *Phys. Rev. Lett.*, 92(23):235003–+, 2004.

[5] K. H. Burrell, T. E. Evans, E. J. Doyle, M. E. Fenstermacher, R. J. Groebner, A. W. Leonard, R. A. Moyer, T. H. Osborne, M. J. Schaffer, P. B. Snyder, P. R. Thomas, W. P. West, J. A. Boedo, A. M. Garofalo, P. Gohil, G. L. Jackson, R. J. La Haye, C. J. Lasnier, H. Reimerdes, T. L. Rhodes, J. T. Scoville, W. M. Solomon, D. M. Thomas, G. Wang, J. G. Watkins, and L. Zeng. ELM suppression in low edge collisionality H-mode discharges using n = 3 magnetic perturbations. *Plasma Physics and Controlled Fusion*, 47:B37–B52, 2005.

[6] S. P. Hirshman and J. C. Whitson. Steepest-descent moment method for three-dimensional magnetohydrodynamic equilibria. *Phys. Fluids*, 26(12):3553–3568, 1983.

[7] M. Drevlak, D. Monticello, and A. Reiman. Pies free boundary stellarator equilibria with improved initial conditions. *Nucl. Fusion*, 45(7):731, 2005.

[8] H.J. Gardner. Diagnostic coils on the w vii-as stellarator using a three-dimensional equilibrium code. *Nucl. Fusion*, 30(8):1417–1424, 1990.

[9] V.D. Shafranov and L.E. Zakharov. Use of the virtual-casing principle in calculating the containing magnetic field in toroidal plasma systems. *Nucl. Fusion*, 12:599–601, 1972.

[10] S A Lazerson. The virtual-casing principle for 3d toroidal systems. *Plasma Physics and Controlled Fusion*, 54(12):122002, 2012.

[11] James D. Hanson, Steven P. Hirshman, Stephen F. Knowlton, Lang L. Lao, Edward A. Lazarus, and John M. Shields. V3fit: a code for three-dimensional equilibrium reconstruction. *Nuclear Fusion*, 49(7):075031, 2009.

[12] T Yamaguchi, K Y Watanabe, S Sakakibara, K Ida, Y Narushima, K Narihara, K Tanaka, T Tokuzawa, M Yoshinuma, T Kobuchi, I Yamada, K Kawahata, H Yamada, and LHD Experimental Group. The effect of net toroidal current on the measurement of diamagnetic beta value in heliotron plasma. *Plasma Physics and Controlled Fusion*, 48(9):L73, 2006.

[13] T Yamaguchi, K Y Watanabe, S Sakakibara, Y Suzuki, Y Narushima, K Narihara, T Tokuzawa, K. Tanaka, I Yamada, H Yamada, K Kawahata, and LHD Experimental Group. New calibration method of magnetic measurements based on the mhd equilibrium with the ergodic region. *Plasma Fusion Res.*, 1(11), 2006.

[14] A. Komori, H.Yamada, S. Imagawa, O.Kaneko, K. Kawahata, K Mutoh, N Ohyabu, Y. Takeiri, K. Ida, T. Mito, Y.Nagayma, S. Sakakibara, R Sakamoto, T. Shimozuma, K.Y. Watanabe, and O. Motojima. Goal and achievements of large helical device project. *Fusion Sci. and Tech.*, 58(1):1–11, 2010.

[15] S. Sakakibara, H. Yamada, and the LHD Experimental Group. Magnetic Measurements in LHD. *Fusion Sci. and Tech.*, 58:471–481, 2010.

[16] J.D. Hanson and S.P. Hirshman. Compact expressions for the biot-savart fields of a filamentary segment. *Phys. of Plasmas*, 9(10):4410–4412, 2002.

[17] Kenji Harafuji, Takaya Hayashi, and Tetsuya Sato. Computational study of three-dimensional magnetohydrodynamic equilibria in toroidal helical systems. *Journal of Computational Physics*, 81(1):169 – 192, 1989.

[18] Yasuhiro Suzuki, Noriyoshi Nakajima, Kiyomasa Watanabe, Yuji Nakamura, and Takaya Hayashi. Development and application of hint2 to helical system plasmas. *Nuclear Fusion*, 46(11):L19, 2006.

The Princeton Plasma Physics Laboratory is operated
by Princeton University under contract
with the U.S. Department of Energy.

Information Services
Princeton Plasma Physics Laboratory
P.O. Box 451
Princeton, NJ 08543

Phone: 609-243-2245
Fax: 609-243-2751
e-mail: pppl_info@pppl.gov
Internet Address: http://www.pppl.gov